Journal of Experimental Botany, Vol. 64, No. 11, pp. 3483–3497, 2013
doi:10.1093/jxb/ert184 Advance Access publication 4 July, 2013
This paper is available online free of all access charges (see http://jxb.oxfordjournals.org/open_access.html for further details)

Journal of Experimental Botany
www.jxb.oxfordjournals.org

RESEARCH PAPER

The conformational bases for the two functionalities of 2-cysteine peroxiredoxins as peroxidase and chaperone

Janine König, Helena Galliardt, Patrick Jütte, Simon Schäper, Lea Dittmann and Karl-Josef Dietz*

Biochemistry and Physiology of Plants, Bielefeld University, 33501 Bielefeld, Germany

* To whom correspondence should be addressed. Email: karl-josef.dietz@uni-bielefeld.de

Received 29 April 2013; Revised 24 May 2013; Accepted 28 May 2013

Abstract

2-Cysteine peroxiredoxins (2-CysPrxs) are ubiquitous and highly abundant proteins that serve multiple functions as peroxidases, chaperones, and thiol oxidases and in redox-dependent cell signalling. The chloroplast protein plays a role in seedling development and protection of the photosynthetic apparatus. This study aimed to unequivocally link conformation and function. To this end, a set of non-tagged site-directed mutagenized At2-CysPrx variants was engineered, which mimicked the conformational states and their specific functions: hyperoxidized form (C54D), reduced form (C54S, C176S), oxidized form (C54DC176K), phosphorylated form (T92D), reduced ability for oligomerization by interfering with the dimer–dimer interface (F84R) and a C-terminally truncated form [ΔC (–20 aa)]. These variants were fully or partly fixed in their quaternary structure and function, respectively, and were analysed for their conformational state and peroxidase and chaperone activity, as well as for their sensitivity to hyperoxidation. The presence of a His_6-tag strongly influenced the properties of the protein. The ΔC variant became insensitive to hyperoxidation, while T92D and F84R became more sensitive. The C54D variant revealed the highest chaperone activity. The highest peroxidase activity was observed for the F84R and ΔC variants. Efficient interaction with NADP-dependent thioredoxin reductase C depended on the presence of Cys residues and the C-terminal tail. The results suggest that the structural flexibility is important for the switch between peroxidase and chaperone function and that evolution has conserved the functional switch instead of maximizing a single function. These variants are ideal tools for future conformation-specific studies *in vivo* and *in vitro*.

Key words: Chaperone, chloroplast, conformation, peroxidase, peroxiredoxin, thiol switch.

Introduction

2-Cysteine peroxiredoxins (2-CysPrxs) are ubiquitous proteins with conserved functions in all kingdoms of life (Dietz, 2011; Edgar *et al.*, 2012). Additionally, in most organisms the 2-CysPrx homologues are highly abundant proteins. In the erythrocyte, Prdx2 is the third most abundant protein (Wood *et al.*, 2003). In the chloroplast stroma, the two 2-CysPrxs A and B are placed at the 14th and 16th positions in the list of most abundant proteins, respectively (Peltier *et al.*, 2006). The accumulation of hyperoxidized Prxs is a conserved marker of circadian rhythmicity (Edgar *et al.*, 2012). Prx proteins are linked to human diseases; for example, they are key initiators of post-ischaemic inflammation in the brain (Shichita *et al.*, 2012) and play a role in cancer (Neumann *et al.*, 2003; Kim *et al.*, 2008; Chen *et al.*, 2010) and Alzheimer's disease (Yoshida *et al.*, 2009).

2-CysPrxs display at least four functions, namely as a peroxidase, chaperone, thiol oxidase, and modulator of cell signalling. Essential for the peroxidase function is the highly reactive cysteinyl residue in the active site (peroxidatic Cys, Cys_P), which reacts with a broad range of hydroperoxides and peroxynitrite (Dietz, 2011). The intermediately formed sulfenic acid of Cys_P reacts with a second cysteine thiol (resolving Cys, Cys_R) from the other subunit of the homodimer to build a disulfide bridge. This oxidized disulfide form is regenerated

Abbreviations: 2-CysPrx, 2-cysteine peroxiredoxin; CDSP32, chloroplast drought-specific protein of 32 kDa; CS, citrate synthase; NTRC, NADPH-dependent thioredoxin reductase with built-in thioredoxin domain; Prx, peroxiredoxin; Srx, sulfiredoxin; TR, thioredoxin reductase; Trx, thioredoxin.

by several chloroplastic thioredoxins (Trxs) and proteins with Trx domains, in particularly NADPH-dependent Trx reductase (TR) with a built-in Trx domain (NTRC), *in vitro* and *in vivo* (Pulido *et al.*, 2010). However, the sulfenic acid intermediate is susceptible to further oxidation to sulfinic acid. Cys_P hyperoxidation switches the function from peroxidase to that of a chaperone. Furthermore, accumulation of the hyperoxidized form shows rhythmicity along with the circadian clock in algae, humans, and plants (O'Neill *et al.*, 2011; Edgar *et al.*, 2012) and coincides with membrane association (König *et al.*, 2003). A high peroxide concentration and lipid hydroperoxides are contributing factors. Additionally, the decameric form of 2-CysPrx is linked to the chaperone function (Jang *et al.*, 2004; Kim *et al.*, 2009). The molecular basis for the functional switch from peroxidase to chaperone is still not completely understood. Sulfiredoxins (Srxs) reduce the hyperoxidized protein in a Mg^{2+}/ATP/thiol reductant-dependent reaction. Due to the limited Srx concentration and slow reaction rate, the regeneration of hyperoxidized 2-CysPrx *in vivo* is a slow process (Iglesias-Baena *et al.*, 2010).

2-CysPrxs have been suggested to function as a redox-dependent molecular hub within the redox regulatory network. Besides Trx and Trx-like proteins, cyclophilin (Cyp20-3), Srx, fructose-1,6-bisphosphatase, and photosystem II were reported as interacting partners of 2-CysPrx in plants (Caporaletti *et al.*, 2007; Laxa *et al.*, 2007; Muthuramalingam *et al.*, 2009). In addition to the peroxidase and chaperone functions, a role as proximity-based thiol oxidase has been proposed (Gutscher *et al.*, 2009). A precise understanding of the relative significance of these different roles of 2-CysPrx *in vivo* is still missing, but they are all in line with the suggested role of Prxs as redox sensors within the thiol-disulfide redox regulatory network of the cell (Dietz, 2008).

This work aimed to dissect the functional diversity and link the quaternary structure 2-CysPrx to its specific functions. To this end, 2-CysPrx variants were designed that were sought to mimic distinct quaternary structures and redox states. Fixing the conformation by introducing defined amino acid exchanges should then allow using the variants as gain-of-function tools to investigate their activities and properties undisturbed from redox changes during the catalytic cycle. To this end, the quaternary structure and peroxidase and chaperone activities, as well as the hyperoxidation sensitivity, were analysed for a set of site-directed mutagenized variants. It was shown that, for such an investigation of fine-tuned functional differentiation, non-tagged variants need to be used, as His_6-tagged 2-CysPrx displayed behaviour in some assays different from the non-tagged protein. Analyses of the variants suggested that the flexibility of the protein structure is essential for its sensitivity to hyperoxidation and for the switch from the peroxidase to chaperone function.

Materials and methods

Cloning, expression, and purification of proteins

The gene sequence of 2-CysPrxA (At3g11630) was amplified by PCR from cDNA of *Arabidopsis thaliana* (Columbia) without the signal peptide (N-terminal MAQA) using a forward primer containing an *Nde*I site and a reverse primer containing an *Eco*RI site. The PCR product was cloned into the *Nde*I/*Eco*RI site of pCRT7/NT-TOPO (Invitrogen) and pET-28a (Merck Millipore). In a similar manner, NTRC was cloned into pET-28a. Site-directed mutagenesis was accomplished by PCR using primers as listed in Supplementary Table S1 (at *JXB* online) and verified by sequencing (Eurofins MWG Operon, Eberswalde, Germany).

The plasmids were transformed into *Escherichia coli* BL21(DE3) pLysS, and protein expression was induced with 0.4 mM IPTG at an optical density of 0.45–0.6. After incubation overnight at room temperature, the culture was centrifuged at 5000*g* for 20 min. The pellet was stored at –80 °C.

For purification of non-tagged 2-CysPrx wild type (WT) and variants, the pellets from 1 litre cultures were resuspended in 50 ml of lysis buffer (40 mM Bis-Tris/HCl, pH 6.5). After 30 min incubation on ice, the bacteria were lysed by sonication (4 × 2 min, 70% power) and centrifuged at 50 000*g* for 45 min. The supernatant was filtered and loaded on a 5 ml HiTrap Q-Sepharose Fast Flow column (GE Healthcare, München, Germany) equilibrated with 40 mM Bis-Tris/HCl (pH 5.5). Proteins were eluted in a 0–1 M sodium acetate gradient with a flat gradient between 30 and 70%. Samples from the protein-containing fractions were analysed by 15% SDS-PAGE. 2-CysPrx-containing fractions were pooled. The 35–80% $(NH_4)_2SO_4$ precipitate was resuspended in 25 mM HEPES/KOH (pH 8.0) and dialysed against the same buffer overnight. Finally, the protein was purified by gel filtration using a S200 16/60 column (GE Healthcare), equilibrated in 40 mM potassium phosphate buffer (pH 7.2). Pooled 2-CysPrx fractions were concentrated using a Vivaspin 20 5000 MWCO centrifugal concentrator (Sartorius, Göttingen, Germany). The protein was frozen in liquid N_2 and stored at –80°C. The protein concentration was determined using the extinction coefficient: ε=19940 M^{-1} cm^{-1} and a theoretical M_w of 22 170 Da (http://expasy.org/tools/protparam.html).

All His-tagged proteins (His_6–2-CysPrx, His_6–NTRC, His_{10}–EcTrxA, and His_{10}–EcTR; König *et al.*, 2002) were purified by Ni-NTA affinity chromatography as described by the manufacturer (Qiagen). The calculated parameters of His_6–NTRC were: M_W=52 282 Da and ε=40715 M^{-1} cm^{-1}.

Quaternary structure analysis

2-CysPrx protein (2 ml at 5 mg ml^{-1}) was loaded on a SEC S200 16/60 (GE Healthcare), or 0.5 ml was loaded on a SEC S200 10/300 GL (GE Healthcare). The column was equilibrated with 40 mM potassium phosphate buffer (pH 7.2). The elution profile was monitored at an optical density of 280 nm.

Peroxidase assay

The standard assay employed *E. coli* Trx as regenerant. 2-CysPrx was added at 2 µM concentration in quartz cuvettes, and the assay was performed at 25°C in 40 mM potassium phosphate buffer (pH 7.2), 1 mM EDTA, 250 µM NADPH, 6–12 µM *E. coli* Trx and 10 µM *E. coli* TR. The reaction was started by the addition of 75 µM H_2O_2, and the decrease in absorbance due to the oxidation of NADPH was measured at 340 nm with a Cary 300 Bio UV/Vis spectrometer (Varian, Middelburg, The Netherlands) for 10 min. Rate constants were determined using the Dalziel equation (Nogoceke *et al.*, 1997; König and Fairlamb, 2007).

Peroxidase assay with dithiothreitol (DTT)

Reduction of H_2O_2 by 2-CysPrx was measured using a ferrous ammonium sulphate/xylenol orange (FOX) assay for H_2O_2 quantification. The assay was performed at 25 °C and contained 40 mM potassium phosphate buffer (pH 7.2), 1 mM DTT, and 5 µM protein (2-CysPrx, His_6-tagged 2-CysPrx, C176S and F84R). After 10 min, the reaction was started by addition of 100 µM H_2O_2. A volume of 10 µl of the assay was added to 200 µl xylenol orange solution

(250 mM sulfuric acid, 1 M sorbitol, 2.5 mM ferrous ammonium sulfate, and 1.25 mM xylenol orange in H_2O) after different time points (0.5, 1, 2, 3, 4, and 5 min). The decrease in H_2O_2 levels was determined spectrophotometrically by measuring absorbance at 560 nm.

Inactivation assay

The reaction conditions were identical to the Trx-dependent peroxidase assay described above with 15 µM *E. coli* Trx. NADPH oxidation was started after addition of 0.25, 1, 2, 5, and 10 mM cumene hydroperoxide, and the decrease in absorbance due to NADPH oxidation was determined by measuring absorbance at 340 nm for 5 min. Background H_2O_2 reduction without 2-CysPrx was subtracted. The NADPH consumption and consequently the catalytic turnover per 2-CysPrx molecule at each time point were calculated. The turnover numbers were plotted against the time and the resulting curve fitted to a first-order equation (1) with simple weighting:

$$y(t)=A_\infty\,(1-\mathrm{e}^{-kt})$$

The calculated limits were plotted against the cumene hydroperoxide concentration and fitted to an equation describing a single exponential decay curve with offset and statistical weighting:

$$y\,(t)=A_0\,(\text{overall limit of turnover})\times\mathrm{e}^{(-k[\mathrm{COOH}],)}+\text{offset}$$

Chaperone assay

The chaperone activity of 2-CysPrx WT and variants was measured using citrate synthase as substrate. 2-CysPrx protein (10 µM) was incubated at 45 °C in 40 mM potassium phosphate buffer (pH 7.2). After temperature adjustment for 15 min, citrate synthase (1 µM) was added and the increase in absorption at 360 nm was monitored with a spectrophotometer.

Circular dichroism (CD) spectra

CD spectra of 10 µM 2-CysPrx protein solutions in 100 mM potassium phosphate buffer (pH 8) and 5 mM NaCl were measured at 20 °C with a quartz microcuvette (light path 0.2 × 1 cm) placed in a J-810 spectropolarimeter (Jasco, Easton, MD, USA). Spectra were measured at a 1 nm data pitch and a scanning speed of 50 nm min^{-1} and averaged over four scans. Four spectra for each condition were collected and averaged after subtracting the base line with buffer only. For quantification of secondary structures, the ellipticity of CD spectra was analysed with the software Spectra Manager (Jasco). CD spectra were compared between oxidized and reduced proteins. 2-CysPrx WT and variants were reduced in 100 mM potassium phosphate buffer (pH 8) and 5 mM NaCl with 10 mM DTT at 37 °C for 2 h. The proteins were then dialysed overnight in 100 mM potassium phosphate buffer (pH 8) and 5 mM NaCl supplemented with 1 mM DTT.

Isothermal titration microcalorimetry

2-CysPrx variants were reduced in 40 mM potassium phosphate buffer (pH 8) with 10 mM DTT at 37 °C for 2 h and dialysed overnight in 40 mM potassium phosphate buffer (pH 8), supplemented with 1 mM DTT. All samples were filter sterilized. A VP-ITC (isothermal titration calorimetry) microcalorimeter was adjusted to the following parameters: 25 °C, 10 µcal s^{-1} reference power, initial offset 60 s, stirring speed 502, fast feedback mode, and ITC equilibration option. Protein was loaded in the syringe, the ITC cuvette was filled with dialysis buffer and 120 nmol of protein was injected in an interval of 3 min (Barranco-Medina *et al.*, 2008).

Far-Western dot blot

2-CysPrx protein (5 µl of 0.63, 1.25, 2.5, 5, 10, and 20 µM, WT and variants) was spotted in arrays on nitrocellulose membrane. Following washing in TBS/Tween 20 (TBST) and 1 h of blocking (1% skimmed milk in TBST), the membrane was equilibrated in binding buffer [50 mM MOPS (pH 6.5), 20% glycerol, 2 mM DTT, 10 mM $MgCl_2$] containing 20 µg ml^{-1} of NTRC. Following repeated washing in TBST, the primary antibody (mouse anti-His_6, diluted 1:6000 in blocking solution) was incubated for 3 h. After washing, alkaline phosphatase-conjugated secondary antibody was added for 2 h. Alkaline phosphatase activity was quantified on the membrane in 30 ml carbonate buffer (pH 9) containing BCIP/NBT following digitization of the images and using image analysis software. The background signal of neighbouring membrane sections without protein was routinely subtracted. Staining intensities were linear in the concentration range from 1.25 to 10 µM for each variant. NTRC binding of the variants at each concentration was calculated in relation to WT (100%). Finally, NTRC binding was presented as mean±standard deviation (SD) at protein concentrations ranging from 1.25 to 10 µM.

Results

Engineering of 2-CysPrx variants

The aim of the work was to engineer and characterize 2-CysPrx variants mimicking naturally occurring 2-CysPrx conformations. These variants should have fixed quaternary structures or restricted dynamics, which would allow the establishment of firm redox-dependent structure/function relationships. Table 1 shows a compilation of all the variants used in this study, outlining the intended functional or structural characteristics. The decameric quaternary structure of reduced 2-CysPrx was fixed by substituting serine for either Cys_P or Cys_R as shown previously for barley 2-CysPrx (König *et al.*, 2003) (Supplementary Fig. S1 at *JXB* online). The variant lacking Cys_R (C176S) should have enhanced proximity-based thiol oxidase capacity as a consequence of the expanded life time of the sulfenic acid intermediate (Gutscher *et al.* 2009). Substitution of Cys_R (C176S) should affect the interaction with Trx-like proteins (König *et al.*, 2003). The negative charge introduced during sulfinic acid formation in the hyperoxidized 2-CysPrx might be simulated by the negatively charged aspartic acid (C54D). This type of site-directed mutagenesis is often used to functionally mimic thiol hyperoxidation (Wang *et al.* 2012). The oxidized 2-CysPrx forms a disulfide bridge between Cys_P and Cys_R.

Table 1. *2-CysPrx variants generated and characterized in this study*

2-CysPrx variant	Mimicked 2-CysPrx conformation
Wild type (WT)	Redox-variable conformation
C54D	Hyperoxidized form
T92D	Phosphorylated form
C54S	Reduced form, interaction with Trx-like proteins
C176S	Reduced form with putative thiol oxidase function
ΔC (–15 aa)	Peroxidase with a loss of sensitivity to hyperoxidation
C54DC176K	Oxidized form
F84R	Reduced aggregation capacity, increased sensitivity to hyperoxidation
WT, N-6×His	Enhanced flexibility by limited steric constraints

Here, a salt bridge between aspartic acid and the positively charged lysine was hypothesized to imitate the oxidized disulfide form (C54DC176K). Introducing the Lys–Asp salt bridge instead of Cys208 and Cys272 successfully restored the disulfide-dependent state of CadC, a regulator of *E. coli* gene expression (Tetsch *et al.* 2011). The C-terminal tail of one homodimer subunit embraces the other subunit and the redox cycle of 2-CysPrx involves extensive changes in quaternary structure. A shortened C-terminal tail should increase the flexibility and the speed of the change in quaternary structure during the catalytic cycle and affect the sensitivity to hyperoxidation. The homologue of tryptophane residue W180 was shown to be essential for the quaternary structure in barley 2-CysPrx (König *et al.*, 2003). The neighbouring lysine residue (K181) potentially forms a salt bridge with a negatively charged amino acid residue near the catalytic centre, thereby stabilizing the loop that contains Cys_R (Supplementary Fig. S1). The remaining residues of the C terminus should be less important for the peroxidase activity and therefore a variant lacking the last 20 aa was designed (ΔC). The stability of the dimer–dimer interface in 2-CysPrxs is mainly based on hydrophobic interactions (Matsumura *et al.*, 2008). Replacing the hydrophobic Phe by a charged residue in this interface should impede the interaction in the dimer–dimer interface and stabilize the dimeric form (F84R). Recently, it was found that *Oryza sativa* 2-CysPrx is phosphorylated (Chen *et al.*, 2011). Plant 2-CysPrxs have the conserved threonine residue T92. This residue is also found in other organisms (Supplementary Fig. S1). In a human cell line, the threonine residue was found to be phosphorylated as well. Human Prdx1 variant T90D eluted only in the fraction containing high-molecular-weight protein (Jang *et al.*, 2006). Prdx1 T90D displayed very low peroxidase activity and showed markedly increased chaperone activity. The variant T92D where aspartic acid replaces threonine should simulate the negative charge introduced by threonine phosphorylation. N-terminally His_6-tagged 2-CysPrx has been used in nearly all studies without thorough testing of whether the charged tag affects the conformational dynamics, catalytic activities or redox-linked properties. As we were interested in major but also subtle modifications, the influence of the His_6 tag was investigated in parallel.

Cloning, expression, and purification

The bioinformatics-predicted plastid transit peptide consists of 82 aa (TargetP) starting with the amino acids MAS/C (Supplementary Fig. S1). Mass spectrometric data of At-2-CysPrx available in the Plant Proteome Database (PPDB, http://ppdb.tc.cornell.edu/) as well as N-terminal sequencing of the pea 2-CysPrx suggest the N-terminal cleavage of the 2-CysPrx signal peptide before Ala67 (AQA…) (Caporaletti *et al.*, 2007). Therefore, tag-free 2-CysPrx was expressed starting with the N-terminal amino acids MAQA. WT and variants were expressed heterologously in *E. coli* with high yield. WT 2-CysPrx was also expressed with an N-terminal His_6-tag. The calculated low isoelectric point of pI=4.91 of 2-CysPrx A was exploited for a first efficient purification step by anion exchange chromatography. All variants were isolated with purities >90% after this step. Following ammonium sulfate precipitation, a final purification was achieved by size exclusion chromatography. Analysis by SDS-PAGE demonstrated the successful purification of all 2-CysPrx A variants (Fig. 1). In solution, 2-CysPrx forms stable dimers as the smallest unit that can aggregate in solution to form doughnut-shaped decamers. Under reducing and denaturing conditions of SDS-PAGE analysis, the reduced dimer decayed to monomers (22.4 kDa). However, a small fraction of reduced dimers was still seen as dimers (44.8 kDa) (Fig. 1). The oxidized dimers were covalently linked and could be clearly distinguished from the reduced monomer. The variants C54S, C176S, and C54DC176K did not form dimers under reducing and non-reducing conditions. Interestingly, a significant double band of C54D at the size of the dimer was seen in the absence of DTT. It can be speculated that a negative charge in the active site, either due to hyperoxidation to sulfinic acid or here due to the aspartic acid, activated the second cysteine C176 from the same subunit to form a disulfide bridge with other proteins or with another 2-CysPrx C54D dimer. Alternatively, the pseudo-hyperoxidized state might allow for very persistent hydrophobic interactions, which in part are resistant to

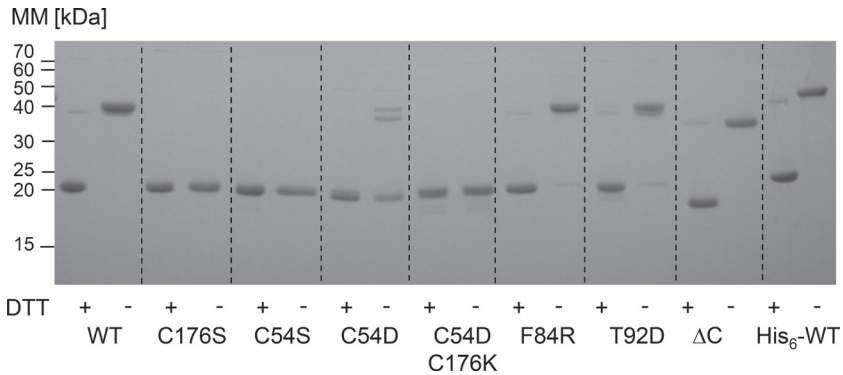

Fig. 1. SDS-PAGE analysis of purified recombinant proteins. All proteins were reduced with 20 mM DTT (+) or left untreated (–) and denatured in loading buffer at 95 °C for 10 min. The redox state was fixed by incubating the proteins with 100 mM *N*-ethylmaleimide. For each lane, 2 μg of each protein was loaded. MM, molecular mass markers (kDa).

SDS during SDS-PAGE separation. N-terminal sequencing could provide definite answers as to a possible truncation of the C54D variant.

Quaternary structure

2-CysPrx undergoes major conformational changes during the catalytic thiol-disulfide and non-catalytic hyperoxidation cycles, respectively (König *et al.*, 2003). Oxidation destabilizes the dimer–dimer interface and causes preferential formation of dimers. Reduction of 2-CysPrx triggers the oligomerization to a doughnut-shaped form, which most often assembles as decamer consisting of five dimers. The elution profile after size fractionation under non-reducing conditions tentatively allowed us to distinguish the dimer eluting at its maximum at 64 ml, the decamer at 46 ml and intermediate or abnormal forms (Fig. 2A). The results could be assigned to three distinct patterns: first, WT, F84R, and the ΔC variants eluted almost exclusively as dimers; secondly, the Cys_P and Cys_R variants C54S and C176S predominantly formed decamers like the reduced protein (Fig. 2A, B) (König *et al.*, 2002). In contrast, the reduced F84R variant eluted as a dimer (Fig. 2B), suggesting that formation of the reduced decamer was impeded in this variant. C54D eluted as an oligomer at 55 ml that was larger than the dimers but smaller than the decamers. The third group contained the salt-bridged C54DC176K and the pseudo-phosphorylated T92D variant, and eluted in a mixed manner as a dimer and decamer.

CD spectra depend on secondary and tertiary structures (Fig. 3, Table 2, and Supplementary Fig. S2 at *JXB* online). The eight variants were analysed for altered CD in the reduced and oxidized state. In all proteins except C54DC176K and C176S, oxidation increased the α-helical proportion at the expense of β-turns and other more random structures. Thus, C54DC176K in the reduced state was already close to the α-helical arrangement realized in the oxidized WT, suggesting at least partial establishment of the salt bridge and an arrangement mimicking the oxidized form. C54D revealed the highest percentage of

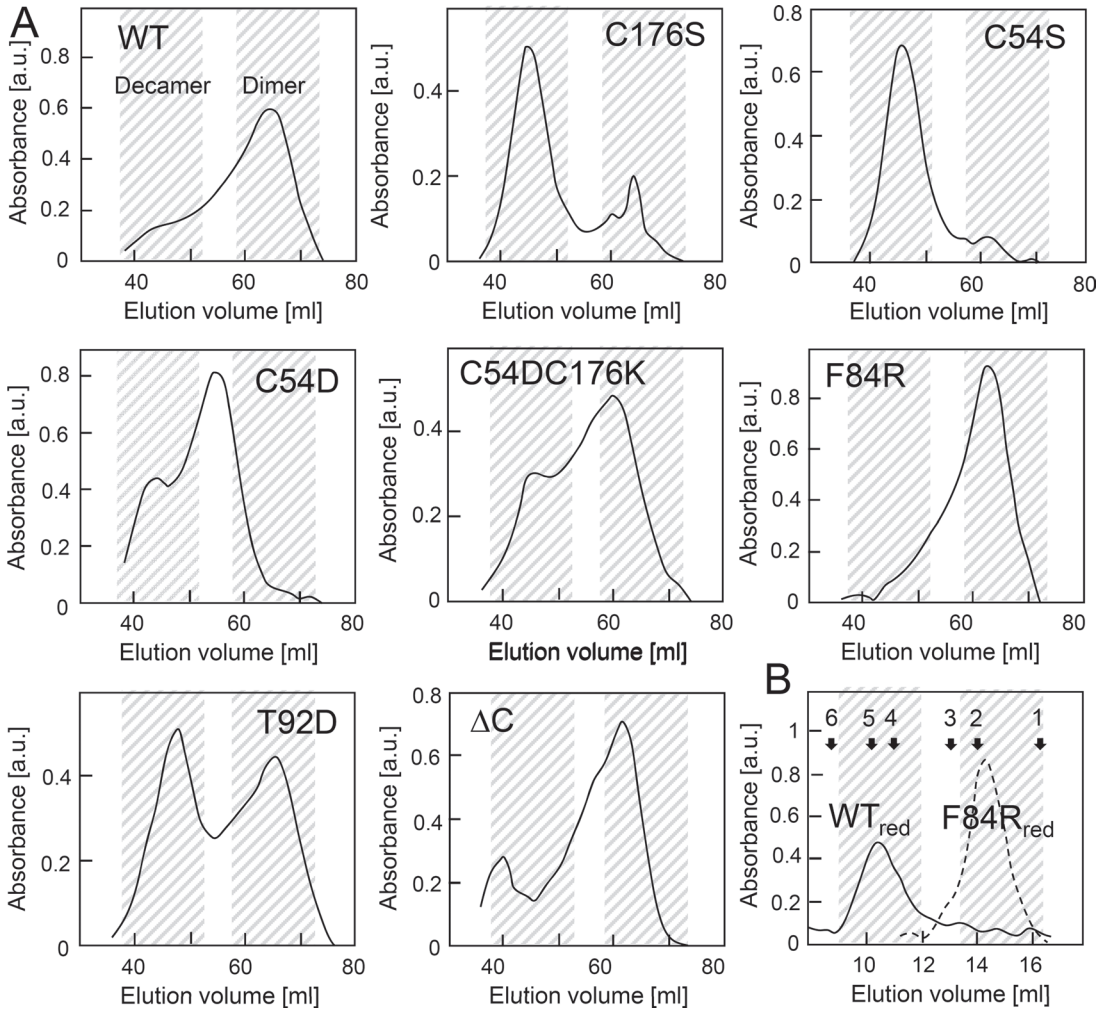

Fig. 2. Size-exclusion chromatography elution profiles of 2-CysPrx WT and variants. (A) Two ml of 5 mg protein ml^{-1} was separated on an S200 16/60 size-exclusion chromatography column using 40 mM potassium phosphate (pH 7.2) as running buffer. (B) 2-Cys Prx WT and F84R were reduced for 2 h with 10 mM DTT and analysed using an S200 10/300 gel filtration column using 40 mM potassium phosphate (pH 7.2) as running buffer. Standard proteins were used for calibration: 1, chymotrypsin (25 kDa); 2, 2-Cys Prx WT_{ox}; 3, ovalbumin (44 kDa); 4, aldolase (158 kDa); 5, 2-Cys Prx C54S; 6, catalase (232 kDa).

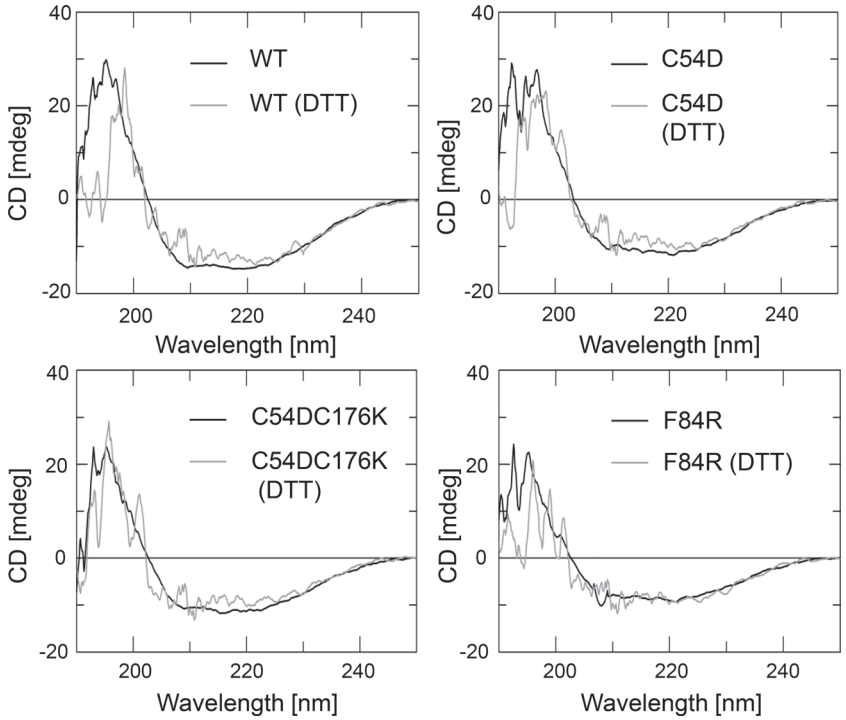

Fig. 3. Secondary structure analysis of 2-CysPrx WT and variants using CD spectroscopy. A concentration of 10 μM non-treated and oxidized and reduced (10 mM DTT) 2-CysPrx WT and variants was analysed. The spectra of the other variants are presented in Supplementary Fig. S2.

Table 2. *Analysis of CD spectra recorded from reduced and oxidized 2-CysPrx*

Data are means±SD of four independent experiments. 2-Cys Prx variants were analysed under non-reducing and reducing conditions. Numbers show the percentage of the respective structures.

	WT	C54D	C54S	C176S	T92D	F84R	C54D/ C176K	ΔC
Non-reducing								
Helix	38±10	57±5	51±4	38±5	38±4	41±3	34±7	80±6
β-sheet	11±3	0±0	0±0	14±8	21±5	19±2	21±7	0±0
Turn	27±3	29±3	39±2	30±3	25±3	22±4	25±1	2±2
Random	24±4	14±3	10±2	18±1	16±2	17±1	19±2	18±4
Reducing								
Helix	28±4	42±0	29±2	33±1	33±9	32±2	31±8	18±3
β-sheet	0±0	2±2	0±0	0±0	6±6	0±0	2±3	61±9
Turn	36±3	40±6	39±7	41±4	37±6	37±4	37±4	6±6
Random	36±6	16±4	32±9	27±5	24±6	31±7	30±10	15±6

helical arrangement among all variants both under reducing and non-reducing conditions, confirming the expectation that introducing the negative charge fosters the compact multimeric state. C176S lacked any redox-dependent change in α-helical assembly, but random and β-turns decreased upon oxidation. This is interesting as it indicates that oxidation of Cys54 triggers a rearrangement of the protein that probably eases disulfide bridge formation. The ΔC variant behaved in a peculiar way as the structure was rearranged upon oxidation in a manner that was much more profound than in any other variant, only approximated by T92D. Apparently a negative charge at aa 92, as possibly introduced by phosphorylation, strongly affects thiol redox-dependent conformational rearrangements. The conformation of the last variant with a charge at the dimer–dimer interface, F84R, was WT-like in the oxidized state but differed from WT as expected in the reduced state where WT 2-CysPrx assembles to oligomers, which was impeded in the F84R variant.

Oligomer–dimer transition by ITC

ITC is a powerful technique to analyse the oligomer–dimer transition of reduced 2-CysPrxs by quantifying the thermodynamics of its dissociation (Barranco-Medina *et al.*, 2008). Only the reduced form displayed this fast dissociation behaviour. The oxidized and hyperoxidized protein showed only background heat dilution. Injected oligomers disintegrate

into dimers below a critical transition concentration (CTC) accompanied by a release of heat; thus, oligomerization is an endothermic reaction. Above the CTC, no dissociation is recorded. Here, the untagged At2-CysPrx displayed a CTC of 3.7 μM, which was about 2.5-fold higher than previously reported for His-tagged At2-CysPrx (Barranco-Medina *et al.* 2008) (Fig. 4, Table 3). The C176S variant showed a lower CTC of 0.63 μM, suggesting that the oligomerized state is stabilized in this variant. The released heat (ΔH) was 22-fold increased in comparison with WT. The C54D variant showed only background heat dilution and no dissociation, and thus a CTC could not be determined.

Peroxidase activity

2-CysPrx reacts with two redox substrates in each reaction cycle, reacting first with the peroxide substrate. Upon Cys_P oxidation, an intermediate sulfenic acid is formed, which then converts to the disulfide bridge with Cys_R. Secondly, the disulfide bridge is reduced by a redox transmitter such as NTRC, Trx-x or CDSP32, to complete the peroxidatic redox cycle. Participation of two substrates implies that the kinetics of 2-CysPrx is well described by a 'ping-pong' mechanism (Nogoceke *et al.*, 1997). Using the integrated Dalziel equation, it is possible to independently determine the rate constants of the hydroperoxide reduction (Fig. 5A) and regeneration by Trx, respectively (Fig. 5B). The best regeneration system of plant 2-CysPrx *in vitro* is the coupled *E. coli* Trx/thioredoxin reductase system (Muthuramalingam *et al.*, 2009) with NADPH as reductant. The regeneration by Trx remained the limiting step during the reaction cycle in all variants irrespective of the introduced modification (Table 4). Both variants with a variation at the N (His_6) or C (ΔC) terminus failed to saturate, and accordingly a V_{max} value could not be determined. The His_6-tagged protein revealed nearly twice the rate constant of hydroperoxide reduction compared

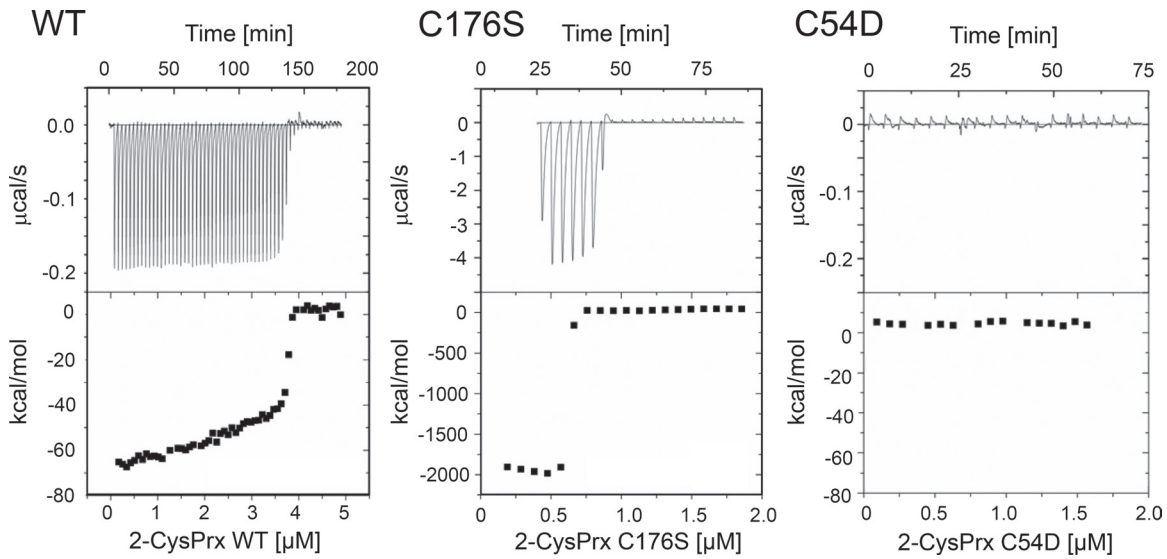

Fig. 4. Quantification of the oligomer–dimer transition by isothermal titration microcalorimetry. Reduced His_6-At2-CysPrx WT forms oligomers which have been shown to disintegrate into dimers below a critical dissociation concentration (CTC) (Barranco-Medina et al., 2008). Here, the thermodynamics of 2-CysPrx dissociation were quantified by multiple injections of highly concentrated reduced 2-CysPrxs (1 mM DTT, 40 mM potassium phosphate) for WT (left panel), C176S (middle panel), and C54D (right panel). The data are summarized in Table 3.

Table 3. *Analysis of 2-CysPrx WT, C54D and C176S dissociation by ITC*

Proteins were titrated under reducing conditions (40 mM potassium phosphate buffer, 1 mM DTT); thus, the protein solubilization buffer and vessel buffer were identical after extensive dialysis. Critical transition concentrations (CTC) and dissociation enthalpy (ΔH_m, kcal/mol) were calculated. Data are means±SD for WT (n=4), C54D (n=6), and C176S (n=5).

2-CysPrx	CTC (μM)	ΔH_m (kcal/mol)
WT	3.73±0.73	72±17
C54D	No dissociation	–
C176S	0.63±0.03	1614±176

with the WT. The reaction rate constant of T92D was indistinguishable from that of WT. The K_M value towards H_2O_2 as well as towards Trx was strongly increased. The hydroperoxide-dependent rate constant of F84R was greatly increased, indicating that the rearrangement of the quaternary structure during transition from dimer to decamer decelerates the reaction in the WT. In a converse manner, the Trx-dependent rate constant was reduced, as was the K_M value towards Trx.

Chaperone function

Previous studies have shown that hyperoxidized 2-CysPrx functions as general chaperone. Citrate synthase (CS)

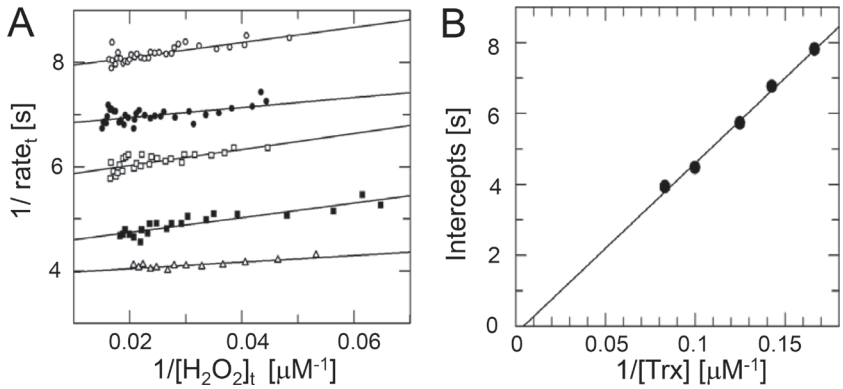

Fig. 5. Kinetic analysis of 2-CysPrx WT and variants. Representative data are shown for WT. Linear plot of the integrated Dalziel rate equation for a two-substrate reaction. Activity of 2-CysPrx was determined with 75 μM hydrogen peroxide and varying concentrations of *E. coli* Trx (6 μM, open circles; 8 μM, filled circles; 10 μM, filled squares; 12 μM, open squares) as described in Materials and methods. (B) Secondary Dalziel plot. The data are summarized in Table 4.

Table 4. *Kinetic properties of 2-CysPrx WT and variants*

Peroxidase activity of the variants that possessed Cys_P was analysed with five different concentrations of EcTrx and 75 μM hydrogen peroxide. The data were analysed using the Dalziel equation. Additionally, the apparent peroxidase activity of 5 μM 2-CysPrx and variants was analysed using 1 mM DTT as reductant and 100 μM hydrogen peroxide. All data are means±SD (n=3). ND, not determined.

2-CysPrx	k_1 (H_2O_2) (10^4 M^{-1} s^{-1})	k_2 (Trx) (10^4 M^{-1} s^{-1})	V_{max} (s^{-1})	K_M (H_2O_2), μM^{-1}	K_M (Trx) (μM)	DTT ($V_{max\ app}$, min^{-1})
WT	3.23±0.02	2.24±0.63	0.38±0.13	12±4	17±1	0.31±0.10
His_6 variant	6.35±1,66	2.26±0.29	>	–	–	1.20±0.07
ΔC	2.64±0,17	2.16±1.15	>	–	–	ND
T92D	2.7±0.6	2.0±0.7	0.52±0.25	83±26	105±24	ND
F84R	8.3±1.0	1.14±0.21	0.70±0.42	8.8±6.1	59±26	0.36±0.04
C176S	ND	ND	ND	ND	ND	0.24±0.10

aggregates at high temperature, as observable by light scattering or as an absorbance change at 360 nm. Hyperoxidized At2-CysPrx protects CS from heat denaturation (Muthuramalingam *et al.*, 2009). Here, in a similar assay, the 2-CysPrx variants were analysed for chaperone activity (Fig. 6, left panel). Only hyperoxidized WT displayed chaperone activity but not the reduced or oxidized protein (Fig. 6, middle panel). The C54D variant showed similar concentration-dependent chaperone activity as the hyperoxidized WT protein, confirming that this variant is mimicking the hyperoxidized protein (Fig. 6, middle panel). Chaperone activity is not just linked to hyperoxidation but was brought into the context of concomitant hyperaggregate formation. Oxidized plant 2-CysPrx exists mainly as a dimer, unlike homologous proteins from other organisms (Cao *et al.*, 2011). The C54D variant predominantly eluted in chromatographic fractions that corresponded to multimers. However, C54D protein from fractions corresponding to low molecular mass as well as from fractions corresponding to the size of an oligomer revealed similar chaperone activity. The other 2-CysPrx variants displayed chaperone activity in a decreasing order of C54D > C176S > C54S > T92D. The C54DC176K and F84R variants lacked any appreciable chaperone activity. Interestingly, 2-CysPrx showed higher chaperone activity using HEPES buffer instead of potassium phosphate buffer (Fig. 6, middle and right panels).

Sensitivity to hyperoxidation

Hyperoxidized 2-CysPrx accumulates *in vivo* as a consequence of severe environmental stress conditions (König *et al.*, 2003). Recently, it was reported that the appearance of hyperoxidized 2-CysPrx may serve as a transcription-independent biomarker for the functional circadian clock (Edgar *et al.*, 2012). Here, an assay was established to quantify the hyperoxidation sensitivity of the variants to get a better understanding of the switch between peroxidase and chaperone activity. Complex hydroperoxides such as cumene hydroperoxide or even more lipid hydroperoxides are known to trigger hyperoxidation (König *et al.*, 2003). 2-CysPrx variants were exposed to various concentrations of cumene hydroperoxide in the presence of the *E. coli* Trx/TR regeneration system. The consumption of NADPH was monitored (Fig. 7A), and the number of cumulated turnovers per 2-CysPrx subunit was calculated (Fig. 7B). The data could be fitted to a saturation curve. The calculated cumulated turnover numbers were plotted against the corresponding cumene hydroperoxide concentrations and the data fitted to an exponential decay curve with offset (Fig. 7C). The ΔC variant maintained very high peroxidase

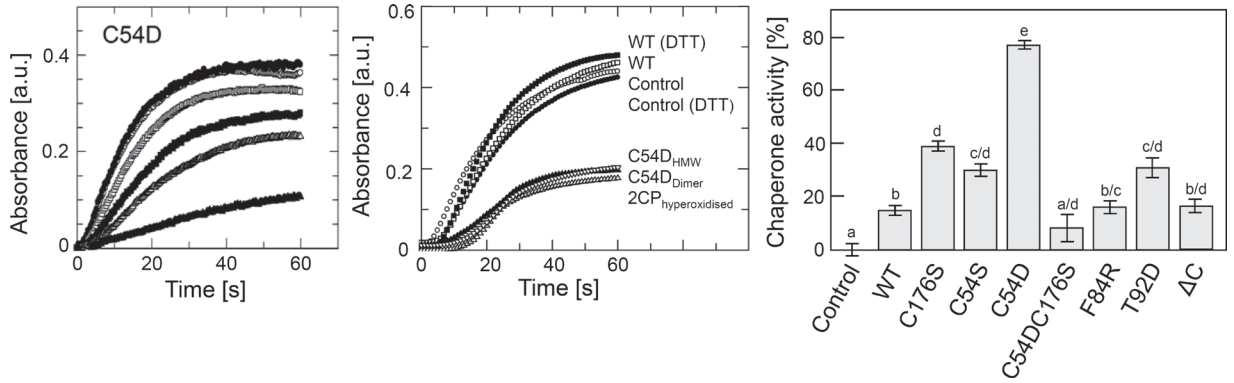

Fig. 6. Chaperone activity. The light scattering due to thermal aggregation at 45 °C of citrate synthase (1 μM) was visualized by using a spectrophotometer at 360 nm. Left panel: chaperone activity of 2-CysPrx C54D in 40 mM potassium phosphate buffer (pH 7.2) at the concentrations of 0 (●), 0.5 (○), 1 (□), 2 (■), 4 (△) and 10 (▲) μM. Middle panel: chaperone activity of oxidized WT (□), reduced WT (■), hyperoxidized WT (△) and non-treated C54D variant at concentrations of 2 μM in 50 mM HEPES buffer (pH 7.0). C54D from fractions eluted by size-exclusion chromatography corresponded to a decamer (▽) or lower molecular mass (▲). The controls contained no 2-CysPrx (○) or 10 mM DTT (●). Right panel: chaperone activities of variants at 10 μM in 40 mM potassium phosphate buffer (pH 7.2). Data are means ±standard error (n=10). Different letters indicate the significance of groups at $P \leq 0.05$ determined using Student's t-test.

activities at high cumene hydroperoxide concentrations, consistent with the lack of saturation (Table 5) already observed in the peroxidase assay. Apparently, the ΔC variant was insensitive to hyperoxidation. The hyperoxidation sensitivity of WT and His_6-tagged protein at very low hydroperoxide concentration was similar, each with a cumulated turnover of about 200 peroxidative cycles per protein subunit. However the rate constant of hyperoxidation was higher than for WT. The offset of over 100 turnovers suggested unspecific hydroperoxide binding, which was seen in the peroxidase assay. The variants T92D and F84R showed considerably decreased cumulated turnover numbers in comparison with WT, and thus high rate constants of hyperoxidation and low offsets. In comparison with F84R, T92D had a higher rate constant and a higher offset, as well as higher K_M values towards cumene hydroperoxide and Trx, respectively.

C176S lacks the Cys_R that is essential for disulfide bridge generation between Cys_P and Cys_R and subsequent regeneration by Trx. The remaining Cys_P in the active site enables hydroperoxide reduction. C176S can be reduced *in vitro* by DTT. With DTT as the reducing agent, the non-tagged C176S displayed a similar peroxidase activity as WT (Table 4). Hyperoxidation of C176S and WT was not detected in this assay. Hyperoxidized 2-CysPrx could be detected by Western blotting using antiserum against sulfinic acid Cys_P. Only His_6-tagged 2-CysPrx was hyperoxidized in the presence of 2 mM H_2O_2 with DTT as reducing reagent (Fig. 7D). The untagged variants were insensitive to hyperoxidation under these conditions.

2-CysPrx variants as tool for analysing the interacting partner

The 2-CysPrx variants are proposed to be instrumental for finding and studying the redox conformation-specific interaction with other proteins. NTRC transfers reducing equivalents to 2-CysPrx (Kirchsteiger *et al.*, 2009; Muthuramalingam *et al.*, 2009; Pulido *et al.*, 2010). *In vivo* studies have shown that NTRC is important for the reduction of 2-CysPrx, especially during the night (Pulido *et al.*, 2010). NTRC is an established interacting partner of 2-CysPrx. Here, the 2-CysPrx variants were used to study the interaction with NTRC by far-Western blot analysis, which is a simple and widely applicable *in vitro* method to assess stable protein–protein interactions (Fig. 8). The 2-CysPrx variants in various concentrations were directly applied on a membrane and incubated with His_6-tagged NTRC. After washing, bound NTRC was detected by immunostaining with anti-oligo-His antibody. The thiol-containing PrxIIE was used as a control for non-specific binding and showed only slight background interaction. WT and the C176S, C54S, C54D and F84R variants showed similar binding of NTRC. All these variants contained at least one cysteine residue, whereas binding of the cysteine-free variant C54DC176K was considerably reduced. Interestingly, binding of the T92D variant was also reduced. The variant with a truncated C-terminal tail showed the lowest binding affinity. The results suggest that both cysteine residues enhance the interaction but that the C-terminal tail is especially important for the NTRC–2-CysPrx interaction.

Discussion

2-CysPrx serves two conserved and thus principle functions as an alkyl hydroperoxide-detoxifying peroxidase and chaperone (Muthuramalingam *et al.*, 2009; König *et al.*, 2012). This work aimed to separate these functions by forcing the protein into specific states. In addition to previously described mutants lacking Cys_P or Cys_R, five novel variants were designed that adopted specific conformational states and thus favoured the peroxidase function

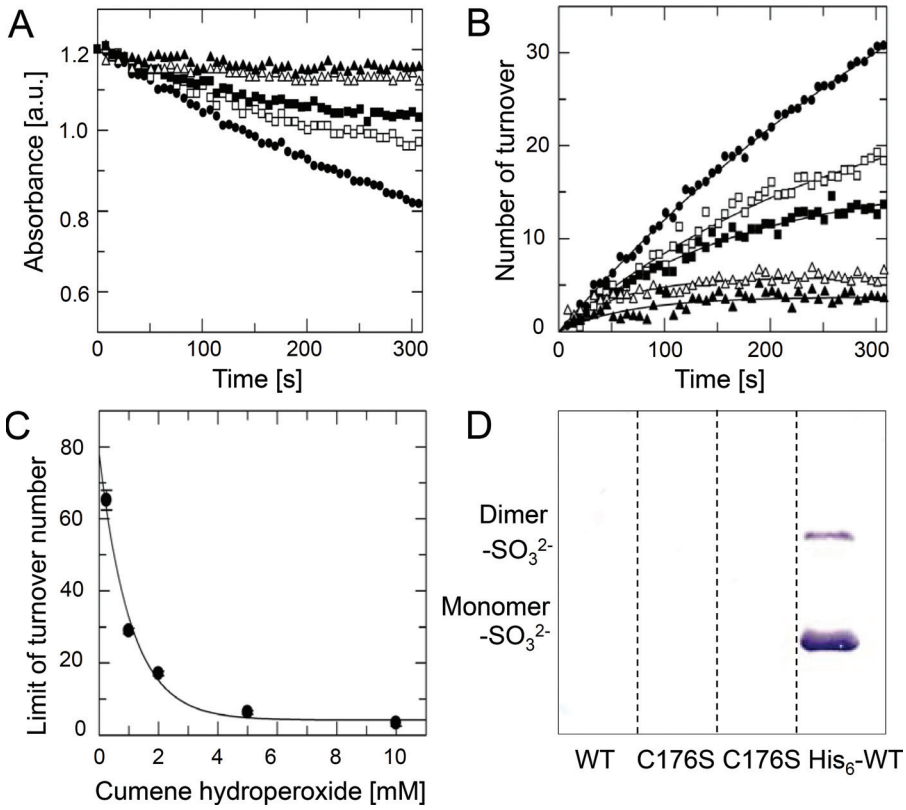

Fig. 7. Hyperoxidation sensitivity of 2-CysPrx WT and variants. Representive data are shown for 2-CysPrx F84R. Similar assay conditions were applied as used for the peroxidase activity. A fixed concentration of 15 μM Ec-Trx was used, and the reaction was started with various concentrations (0.5, 1, 2, 5, and 10 mM) of cumene hydroperoxide. (A) The NADPH consumption was monitored over 5 min. (B) The number of turnovers per 2-CysPrx molecule was calculated and plotted against time. The data were fitted to an equation describing a saturation curve. (C) The calculated limits of turnover were plotted against cumene hydroperoxide concentrations. Data were fitted to an equation describing an exponential curve with offset. The calculated parameters are displayed in Table 5. (D) Western blot analysis of hyperoxidized 2-CysPrx using antiserum against sulfinic acid 2-CysPrx (2-CysPrx-SO_3^{2-}). WT, C176S and His_6-WT were reduced with 10 mM DTT and treated three times with 2 mM H_2O_2 for 15 min at 37 °C. Untreated C176S was loaded in lane 2. One microgram of each 2-CysPrx variant was loaded per lane.

Table 5. *Sensitivity of 2-CysPrx WT and variants to inactivation by hyperoxidation*

The initial rate in the TR/Trx system was determined with 50 μM cumene hydroperoxide (COOH). Data are means ±SD (*n*=3).

2-CysPrx	Initial rate (s^{-1} H_2O_2)[b]	Initial rate (s^{-1} COOH)	Overall limit of turnover	COOH concentration reducing turnover to half (mM)	Offset
WT	0.23 ± 0.01	0.44 ± 0.01	193 ± 35	0.17 ± 0.11	-5.5 ± 51
His_6-	0.26 ± 0.00	0.34 ± 0.01	230 ± 19	0.27 ± 0.07	105 ± 20
ΔC	0.31 ± 0.03	0.38 ± 0.03	>[a]	>[a]	>[a]
T92D	0.14 ± 0.01	0.18 ± 0.01	73 ± 12	1.47 ± 0.37	20.0 ± 2.3
F84R	0.14 ± 0.01	0.19 ± 0.01	74 ± 10	0.95 ± 0.17	4.1 ± 1.3

[a] No inactivation but enhanced peroxidase activity of the ΔC-variant was observed.
[b] The initial rate was determined with 75 μM hydrogen peroxide.

(ΔC), or mimicked the hyperoxidized chaperone (C54D), the oxidized inactive protein (C54DC176K), the reduced dimeric protein, which usually would accumulate only to a concentration of about 1–2 μM (F84R), and the phosphorylated protein (T92D). Fig. 9 provides a summary of the results observed in this study and discussed in the following sections.

Variants as tools for analysing specific conformational states and functions

All catalytically active variants were compared with non-tagged At2-CysPrx WT protein. WT protein showed a peroxidase function with kinetic parameters for H_2O_2 reduction (k_{cat}/K_M: $3.23 \pm 0.02 \times 10^4$ M^{-1} s^{-1}) similar to those described

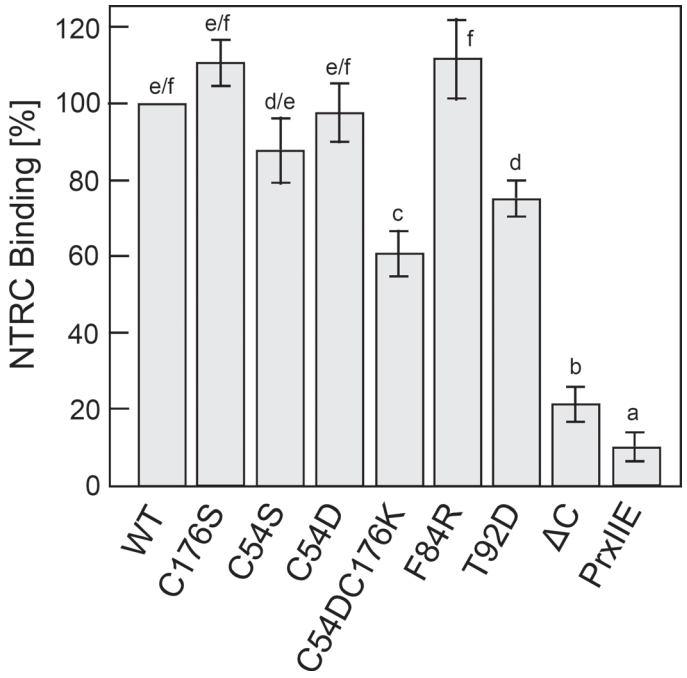

Fig. 8. Interaction of At-NTRC with 2-Cys Prx WT and variants as determined by far-Western blotting. Various 2-Cys Prx variants in six different concentrations were spotted on a nylon membrane. The membrane was overlayed with reduced His_6-NTRC and after several washing steps, the interacting His_6-NTRC was visualized by immunodetection using anti-His_6 antiserum. The experiment was repeated four times. Staining intensity was quantified in digitized images using gel scanning software. Background staining was subtracted. Staining intensities in the linear data range were related to WT (100%). Data represent means±SD (n=4). Different letters indicate the significance of groups at $P \leq 0.05$ determined using Student's t-test.

for *Pisum sativum* 2-CysPrx (k_{cat}/K_M: 2.5×10^4 M^{-1} s^{-1}) (Bernier-Villamor *et al.*, 2004). Like the reduced WT, both mutants lacking Cys_P or Cys_R eluted as decamers after size-exclusion chromatography. This result was in agreement with previous reports for barley 2-CysPrx (König *et al.*, 2002). However, unlike the reduced WT, both variants displayed significant chaperone activity. The C54D variant with its negative charge in the catalytic centre acted as a chaperone, as reported previously for the hyperoxidized human 2-CysPrx (Jang *et al.*, 2004). The C54D oligomer was unable to dissociate like the hyperoxidized His_6-tagged 2-Cys Prx (Barranco-Medina *et al.*, 2008). These results confirmed that the C54D variant mimics the hyperoxidized state and can be used to analyse 2-CysPrx chaperone function.

The C54DC176K variant, which was designed to simulate the oxidized dimer by introducing a salt bridge, displayed no significant chaperone function and, due to the loss of cysteines, no peroxidase function. Size-exclusion chromatography indicated that this variant existed as a mixture of dimers and decamers in solution. Apparently, this variant was at least partly mimicking the oxidized protein, which occurs within the peroxidase cycle. The F84R variant in the oxidized as well as the reduced form showed the dimeric conformation. The protein displayed an enhanced reaction rate constant and a lower K_M value towards hydrogen peroxide, resulting in a higher sensitivity to hyperoxidation. The disturbance of the dimer–dimer interface in the F84R variant destabilized the reduced decamer conformation and facilitated hyperoxidation. The T92D variant displayed a similar peroxidase function and sensitivity to hyperoxidation as the F84R variant. Size-exclusion chromatography analysis suggested that this variant exists as a dimer and various forms of aggregated dimers up to decamers in solution. The peroxidase activity of the ΔC variant was similar to WT at low, *in vivo*-relevant hydroperoxide concentrations. Due to the loss of saturation, the variant displayed strongly increased peroxidase activity at higher hydroperoxide concentrations. In addition, this variant became tolerant to hyperoxidation and displayed no significant chaperone function. The dimeric conformation of the oxidized ΔC variant and the results of catalytic and regeneration rates suggested that elimination of the flexible C terminus converts 2-CysPrx into a more efficient peroxidase. Apparently, the C terminus is the major determinant of the slow peroxidase cycle. Thus, the maintenance of the C-terminal extension appears to be a prerequisite to enable the functional switch from peroxidase to chaperone. Analysis of C-terminally truncated *Schizosaccharomyces pombe* 2-CysPrx has illustrated that the positive charge of the conserved residue Lys191 is a major factor contributing to the hyperoxidation sensitivity (Koo *et al.*, 2002). It was concluded that the optimization of peroxidase function was not a major driving force during evolution.

NTRC–2-CysPrx interaction

NTRC has been shown to efficiently re-reduce oxidized 2-CysPrx *in vitro* (Perez-Ruiz *et al.*, 2006) and *in vivo* (Pulido

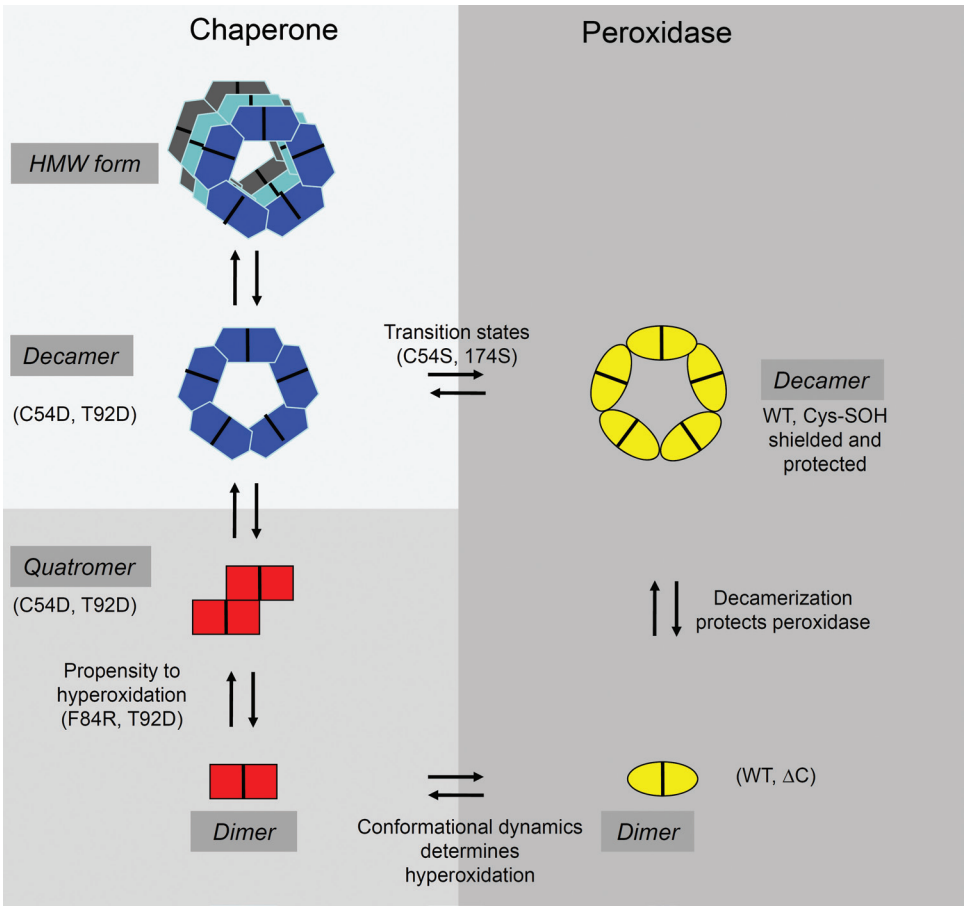

Fig. 9. Summarizing scheme of the results and conclusions. 2-CysPrx adopts two principle different conformations, one with a peroxidase function and one with a chaperone function. The variants introduced in this study arrested certain conformations (C54S, C176S, C54D, C54DC176K, and F84R) and/or modified the flexibility of the protein (ΔC, C176S, and T92D). Hyperoxidation of C54 switches off the peroxidase and switched on the chaperone activity. However, hyperoxidation is not essential for chaperone activity (T92D, C54S, and C176S). This allowed us to suggest the function–structure relationships as indicated in the scheme. See text for further details. (This figure is available in colour at *JXB* online.)

et al., 2010). The interaction is sufficiently strong to be visualized by FRET analysis in transfected protoplasts (Muthuramalingam *et al.*, 2009) and could also be visualized in overlay assays in this work. The interaction was low under reducing conditions for the C54DC176K and ΔC variants. These results concur with the hypothesis that NTRC preferentially interacts with the reduced or hyperoxidized 2-CysPrx and that this interaction is mediated by the C-terminal extension. Association of NTRC with the decameric form and not with the oxidized dimer, as simulated in the C54DC176K variant, could facilitate re-reduction of 2-CysPrx in the regular peroxidase cycle. Under more oxidizing conditions, NTRC might be released from 2-CysPrx in order to preferentially resume other redox regulatory functions (Cejudo *et al.*, 2012). The results exemplarily show that the set of variants constructed in this work should allow straightforward investigation of the molecular basis underlying 2-CysPrx interactions, e.g. with photosystem II, Cyp20-3, or fructose-1,6-bisphosphatase (Laxa *et al.*, 2007; Caporaletti *et al.*, 2007; Muthuramalingam *et al.*, 2009) or other as yet unknown interacting proteins.

Quaternary structure-dependent functions

The reduced WT, C176S and C54D forms all assembled as decamers but showed different CTCs in the ITC dissociation experiment and also different chaperone activities in a reciprocal order. These results support previous suggestions (Barranco-Medina *et al.*, 2008; Muthuramalingam *et al.*, 2009) that there might exist distinct decameric states with different structural and functional properties, namely the reduced decamer favouring peroxidase activity, the decamer with strong chaperone function but in addition intermediate conformational states. The chaperone function of the oxidized T92D variant and non-hyperoxidized C54S and C176S variants implied that the chaperone activity did not necessarily depend on the hyperoxized Cys_P in the protein. Hyperoxidation only represents one possibility for switching the function from peroxidase to chaperone. Furthermore, chaperone activity was not limited to the decameric or high-molecular-weight forms of 2-CysPrx as seen for the C54D and T92D variant. The presented data suggest that there are two principle conformations, which do not depend exclusively

on the dimer or decamer form or on the redox state (Fig. 9). One conformation can be assigned to the chaperone function and the other to the peroxidase function.

Cys_P and Cys_R are spaced about 13 Å apart in the reduced decamer (Cao *et al.*, 2011). This distance is closed upon oxidation, which requires structural flexibility. The dimer–dimer interface is modified in F84R, which impeded decamerization in the reduced state. Exclusive elution of F84R as a dimer during size-exclusion chromatography confirmed this hypothesis. It appears that this disturbance of the dimer–dimer interface with the concomitant permanent adoption of the dimeric conformation eased the accessibility of Cys_P and allowed a faster reaction with hydroperoxides. It may be hypothesized that eased accessibility increases the sensitivity of Cys_P to hyperoxidation compared with the WT, which adopts the decameric form in the reduced state. These observations are in line with the known dynamics of 2-CysPrx in the peroxidase cycle. Hyperoxidation sensitivity of F84R provides an explanation as to why the extremely high cooperativity in decamer formation of the reduced 2-CysPrx (Barranco-Medina *et al.*, 2008; Barranco-Medina *et al.*, 2009) might be beneficial: the rapid decamer assembly lowers the rate of hyperoxidation in the cell. Furthermore, it is hypothesized that the velocity with which the conformational switch occurs between the oxidized dimer and the reduced decamer is the major determinant of the rate of hyperoxidation.

Apparently, the structure of 2-CysPrx is highly flexible. Changes in the redox state of Cys_P and Cys_R strongly affect the equilibrium between the different conformational states. In addition, other post-translational modifications also modulate the functional state of 2-CysPrx and contribute to the switch between peroxidase and chaperone activity. Described mechanisms for human 2-CysPrxs include phosphorylation (Rhee *et al.*, 2012), glutathionylation (Chae *et al.*, 2012), acetylation (Seo *et al.*, 2009) and proteolysis (Koo *et al.*, 2002). It is suggested that post-translational modifications allow the fine-tuning of 2-Cys Prx function *in vivo*. Furthermore, previous studies have suggested that pH, temperature, and salt concentrations influence the conformation (Bernier-Villamor *et al.*, 2004). In a proteomics approach, rice 2-CysPrx was detected as being reversibly phosphorylated, with heat as the trigger of dephosphorylation (Chen *et al.*, 2011). Introduction of a negative charge at Thr92 mimicking phosphorylation increased the sensitivity of 2-CysPrx to hyperoxidation. It is tempting to speculate that phosphorylation and hyperoxidation might be linked *in vivo* to control 2-CysPrx structure and function. There are several indications that the mammalian cell cycle and the circadian network are coupled (Gerard and Goldbeter, 2012). The data presented here suggest that future studies should address the question of whether other interacting molecules and proteins influence this delicate structure–function equilibrium of 2-CysPrx.

Outlook

This study introduced a collection of 2-CysPrx variants that reliably separate the peroxidase and chaperone functions by adopting defined conformations (Table 1). These variants will be valuable tools in future studies and will allow us to address and differentiate the role of 2-CysPrx in cell signalling and antioxidant defence. Our data provide evidence that it is feasible to obtain variants with enhanced peroxidase or chaperone function. However, evolution has favoured a multifunctional 2-CysPrx protein that switches between the high-affinity but low-turnover peroxidase function and the low-efficiency chaperone function. There is a need in plants, but also in mammals and other organisms, to explore the reasons for this delicate multifunctionality beyond the reported positive effects of, for example, overexpression of 2-CysPrx on oxidative stress and heat tolerance (An *et al.*, 2011; Kim *et al.*, 2011).

Supplementary data

Supplementary data are available at *JXB* online.

Supplementary Fig. 1. Multiple sequence alignment of 2-Cys Prx proteins from various organisms.

Supplementary Fig. 2. Secondary structure analysis of 2-CysPrx variants using circular dichroism spectroscopy.

Supplementary Table S1. Primers used for cloning of 2-CysPrx and variants.

Acknowledgements

The work was supported by the Deutsche Forschungsgemeinschaft (DFG, DI 346/14-1).

References

An BC, Lee SS, Lee JT, Hong SH, Wi SG, Chung BY. 2011. Engineering of 2-Cys peroxiredoxin for enhanced stress-tolerance. *Molecules and Cells* **32,** 257–264.

Barranco-Medina S, Kakorin S, Lazaro JJ, Dietz KJ. 2008. Thermodynamics of the dimer–decamer transition of reduced human and plant 2-cys peroxiredoxin. *Biochemistry* **47,** 7196–7204.

Barranco-Medina S, Lazaro JJ, Dietz KJ. 2009. The oligomeric conformation of peroxiredoxins links redox state to function. *FEBS Letters* **583,** 1809–1816.

Bernier-Villamor L, Navarro E, Sevilla F, Lazaro JJ. 2004. Cloning and characterization of a 2-Cys peroxiredoxin from *Pisum sativum*. *Journal of Experimental Botany* **55,** 2191–2199.

Cao ZB, Tavender TJ, Roszak AW, Cogdell RJ, Bulleid NJ. 2011. Crystal structure of reduced and of oxidized peroxiredoxin IV enzyme reveals a stable oxidized decamer and a non-disulfide-bonded intermediate in the catalytic cycle. *Journal of Biological Chemistry* **286,** 42257–42266.

Caporaletti D, D'Alessio AC, Rodriguez-Suarez RJ, Senn AM, Duek PD, Wolosiuk RA. 2007. Non-reductive modulation of chloroplast fructose-1,6-bisphosphatase by 2-Cys peroxiredoxin. *Biochemical and Biophysical Research Communications* **355,** 722–727.

Cejudo FJ, Ferrandez J, Cano B, Puerto-Galan L, Guinea M. 2012. The function of the NADPH thioredoxin reductase C-2-Cys peroxiredoxin system in plastid redox regulation and signalling. *FEBS Letters* **586,** 2974–2980.

Chae HZ, Oubrahim H, Park JW, Rhee SG, Chock PB. 2012. Protein glutathionylation in the regulation of peroxiredoxins: a family of thiol-specific peroxidases that function as antioxidants, molecular chaperones, and signal modulators. *Antioxidants & Redox Signaling* **16,** 506–523.

Chen MF, Lee KD, Yeh CH, Chen WC, Huang WS, Chin CC, Lin PY, Wang JY. 2010. Role of peroxiredoxin I in rectal cancer and related to p53 status. *International Journal of Radiation Oncology, Biology, Physics* **78,** 868–878.

Chen X, Zhang W, Zhang B, Zhou J, Wang Y, Yang Q, Ke Y, He H. 2011. Phosphoproteins regulated by heat stress in rice leaves. *Proteome Science* **9,** 37.

Dietz KJ. 2008. Redox signal integration: from stimulus to networks and genes. *Physiologia Plantarum* **133,** 459–468.

Dietz KJ. 2011. Peroxiredoxins in plants and cyanobacteria. *Antioxidants & Redox Signaling* **15,** 1129–1159.

Edgar RS, Green EW, Zhao YW, *et al.* 2012. Peroxiredoxins are conserved markers of circadian rhythms. *Nature* **485,** 459–465.

Gerard C, Goldbeter A. 2012. Entrainment of the mammalian cell cycle by the circadian clock: modeling two coupled cellular rhythms. *PLoS Computational Biology* **8,** e1002516

Gutscher M, Sobotta MC, Wabnitz GH, Ballikaya S, Meyer AJ, Samstag Y, Dick TP. 2009. Proximity-based protein thiol oxidation by H_2O_2-scavenging peroxidases. *Journal of Biological Chemistry* **284,** 31532–31540.

Iglesias-Baena I, Barranco-Medina S, Lazaro-Payo A, Lopez-Jaramillo FJ, Sevilla F, Lazaro JJ. 2010. Characterization of plant sulfiredoxin and role of sulphinic form of 2-Cys peroxiredoxin. *Journal of Experimental Botany* **61,** 1509–1521.

Jang HH, Kim SY, Park SK, *et al.* 2006. Phosphorylation and concomitant structural changes in human 2-Cys peroxiredoxin isotype I differentially regulate its peroxidase and molecular chaperone functions. *FEBS Letters* **580,** 351–355.

Jang HH, Lee KO, Chi YH, *et al.* 2004. Two enzymes in one: two yeast peroxiredoxins display oxidative stress-dependent switching from a peroxidase to a molecular chaperone function. *Cell* **117,** 625–635.

Kim JH, Bogner PN, Baek SH, Ramnath N, Liang P, Kim HR, Andrews C, Park YM. 2008. Up-regulation of peroxiredoxin 1 in lung cancer and its implication as a prognostic and therapeutic target. *Clinical Cancer Research* **14,** 2326–2333.

Kim MD, Kim YH, Kwon SY, Jang BY, Lee SY, Yun DJ, Cho JH, Kwak SS, Lee HS. 2011. Overexpression of 2-cysteine peroxiredoxin enhances tolerance to methyl viologen-mediated oxidative stress and high temperature in potato plants. *Plant Physiology and Biochemistry* **49,** 891–897.

Kim SY, Jang HH, Lee JR, *et al.* 2009. Oligomerization and chaperone activity of a plant 2-Cys peroxiredoxin in response to oxidative stress. *Plant Science* **177,** 227–232.

Kirchsteiger K, Pulido P, Gonzalez M, Cejudo FJ. 2009. NADPH thioredoxin reductase C controls the redox status of chloroplast 2-Cys peroxiredoxins in *Arabidopsis thaliana*. *Molecular Plant* **2,** 298–307.

König J, Baier M, Horling F, Kahmann U, Harris G, Schurmann P, Dietz KJ. 2002. The plant-specific function of 2-Cys peroxiredoxin-mediated detoxification of peroxides in the redox-hierarchy of photosynthetic electron flux. *Proceedings of the National Academy of Sciences, U S A* **99,** 5738–5743.

König J, Fairlamb AH. 2007. A comparative study of type I and type II tryparedoxin peroxidases in *Leishmania major*. *FEBS Journal* **274,** 5643–5658.

König J, Lotte K, Plessow R, Brockhinke A, Baier M, Dietz KJ. 2003. Reaction mechanism of plant 2-Cys peroxiredoxin. Role of the C terminus and the quaternary structure. *Journal of Biological Chemistry* **278,** 24409–24420.

König J, Muthuramalingam M, Dietz KJ. 2012. Mechanisms and dynamics in the thiol/disulfide redox regulatory network: transmitters, sensors and targets. *Current Opinion in Plant Biology* **15,** 261–268.

Koo KH, Lee S, Jeong SY, Kim ET, Kim HJ, Kim K, Song K, Chae HZ. 2002. Regulation of thioredoxin peroxidase activity by C-terminal truncation. *Archives of Biochemistry and Biophysics* **397,** 312–318.

Laxa M, König J, Dietz KJ, Kandlbinder A. 2007. Role of the cysteine residues in *Arabidopsis thaliana* cyclophilin CYP20-3 in peptidyl-prolyl cis-trans isomerase and redox-related functions. *Biochemical Journal* **401,** 287–297.

Matsumura T, Okamoto K, Iwahara S, Hori H, Takahashi Y, Nishino T, Abe Y. 2008. Dimer–oligomer interconversion of wild-type and mutant rat 2-Cys peroxiredoxin: disulfide formation at dimer-dimer interfaces is not essential for decamerization. *Journal of Biological Chemistry* **283,** 284–293.

Muthuramalingam M, Seidel T, Laxa M, Nunes de Miranda SM, Gartner F, Stroher E, Kandlbinder A, Dietz KJ. 2009. Multiple redox and non-redox interactions define 2-Cys peroxiredoxin as a regulatory hub in the chloroplast. *Molecular Plant* **2,** 1273–1288.

Neumann CA, Krause DS, Carman CV, *et al.* 2003. Essential role for the peroxiredoxin Prdx1 in erythrocyte antioxidant defence and tumour suppression. *Nature* **424,** 561–565.

Nogoceke E, Gommel DU, Kiess M, Kalisz HM, Flohe L. 1997. A unique cascade of oxidoreductases catalyses trypanothione-mediated peroxide metabolism in *Crithidia fasciculata*. *Biological Chemistry* **378,** 827–836.

O'Neill JS, van Ooijen G, Dixon LE, Troein C, Corellou F, Bouget FY, Reddy AB, Millar AJ. 2011. Circadian rhythms persist without transcription in a eukaryote. *Nature* **469,** 554–558.

Peltier JB, Cai Y, Sun Q, Zabrouskov V, Giacomelli L, Rudella A, Ytterberg AJ, Rutschow H, van Wijk KJ. 2006. The oligomeric stromal proteome of *Arabidopsis thaliana* chloroplasts. *Molecular & Cellular Proteomics* **5,** 114–133.

Perez-Ruiz JM, Spinola MC, Kirchsteiger K, Moreno J, Sahrawy M, Cejudo FJ. 2006. Rice NTRC is a high-efficiency redox system for chloroplast protection against oxidative damage. *Plant Cell* **18,** 2356–2368.

Pulido P, Spinola MC, Kirchsteiger K, Guinea M, Pascual MB, Sahrawy M, Sandalio LM, Dietz KJ, Gonzalez M, Cejudo FJ. 2010. Functional analysis of the pathways for 2-Cys peroxiredoxin reduction in *Arabidopsis thaliana* chloroplasts. *Journal of Experimental Botany* **61,** 4043–4054.

Rhee SG, Woo HA, Kil IS, Bae SH. 2012. Peroxiredoxin functions as a peroxidase and a regulator and sensor of local peroxides. *Journal of Biological Chemistry* **287,** 4403–4410.

Seo JH, Lim JC, Lee DY, *et al.* 2009. Novel protective mechanism against irreversible hyperoxidation of peroxiredoxin: Nα-terminal acetylation of human peroxiredoxin II. *Journal of Biological Chemistry* **284,** 13455–13465.

Shichita T, Hasegawa E, Kimura A, *et al.* 2012. Peroxiredoxin family proteins are key initiators of post-ischemic inflammation in the brain. *Nature Medicine* **18,** 911–917.

Tetsch L, Koller C, Dönhöfer A, Jung K. (2011) Detection and function of an intramolecular disulfide bond in the pH-responsive CadC of *Escherichia coli*. *BMC Microbiology* **11,** 74.

Wang Y, Gibney PA, West JD, Morano KA. 2012. The yeast Hsp70 Ssa1 is a sensor for activation of the heat shock response by thiol-reactive compounds. *Molecular Biology of the Cell* **23,** 3290–3298.

Wood ZA, Schroder E, Harris JR, Poole LB. 2003. Structure, mechanism and regulation of peroxiredoxins. *Trends in Biochemical Sciences* **28,** 32–40.

Yoshida Y, Yoshikawa A, Kinumi T, Ogawa Y, Saito Y, Ohara K, Yamamoto H, Imai Y, Niki E. 2009. Hydroxyoctadecadienoic acid and oxidatively modified peroxiredoxins in the blood of Alzheimer's disease patients and their potential as biomarkers. *Neurobiology of Aging* **30,** 174–185.